

Aus dem Institut für Neuropathologie
Zentrum für Neuropathologie und Prionforschung
Institut der Ludwig Maximilians-Universität München

Direktor: Prof. Dr. Jochen Herms

**Early changes in miRNAs expression in a mouse model of
Parkinson`s Disease**

Dissertation
zum Erwerb des Doktorgrades der Medizin an der
Medizinischen Fakultät der
Ludwig-Maximilians-Universität zu München

Jiao Geng

aus

Baoji, Shaanxi, China

2020

Mit Genehmigung der Medizinischen Fakultät
der Universität München

Berichterstatter: Prof. Dr. Jochen Herms

Mitberichterstatter: Priv. Doz. Dr. J.M. Heyn

Dekan: Prof. Dr. med. dent. Reinhard Hickel

Tag der mündlichen Prüfung: 03. 12. 2020

Affidavit

Geng, Jiao

Surname, first name

I hereby declare, that the submitted thesis entitled

Early changes in miRNAs expression in a mouse model of Parkinson`s Disease

is my own work. I have only used the sources indicated and have not made unauthorised use of services of a third party. Where the work of others has been quoted or reproduced, the source is always given.

I further declare that the submitted thesis or parts thereof have not been presented as part of an examination degree to any other university.

Baoji, 04.12.2020

Place, date

Jiao Geng

Signature doctoral candidate

CONTENT

SUMMARY	6
ZUSAMMENFASSUNG	7
INTRODUCTION	9
1. Parkinson's disease	9
2. Alpha-synuclein	10
3. MicroRNAs	12
4. PD mouse models	13
5. Aim of the study	14
MATERIAL AND METHODS	15
1. Animals and housing conditions	15
2. Genotyping	16
3. Total RNA and small RNA isolation	17
3.1 Total RNA isolation	17
3.2 Small RNA isolation	18
4. Concentration measurement of double strand DNA (ds DNA)	18
5. Western blot	19
6. MiRNA sequencing	21
6.1 Adapters Ligation	22
6.2 cDNA template preparation (Reverse Transcription and PCR)	22
6.3 Quality control of the samples	23
6.4 Size Fractionation (gel purification of cDNA)	24
6.5 Denature and dilute the sample	25
6.6 Sequencing on the Illumina platform	25
7. Data processing	26
RESULTS	27
1. α -syn expression identification in PDGF mice	27
2. Analysis of miRNA expression in PDGF mice	28
2.1 Quality control of cDNA fragments for each sample	29
2.2 Data analysis after miRNA sequencing	30
2.2.1 Prediction of overall similarity and difference between each sample	30
2.2.2 Differential expression of miRNAs in PDGF mice at different time points	31

2.2.2.1 General assessment of miRNAs' differential expression between 2-month-old mice and the other PDGF mice	32
2.2.2.2 Differential expression of miRNAs in PDGF mice between each group (2, 3, 4 months)	34
2.2.2.2.1 Comparison between 3 and 2 months old PDGF mice	34
2.2.2.2.2 Comparison between 4 and 3 months old PDGF mice	35
2.2.2.2.3 Comparison between 4 and 2 months old PDGF mice	36
DISCUSSION	38
1. Differential expression of miRNAs between 2-month-old mice and the PDGF mice of 3 and 4 months of age	38
2. Differential expression of miRNAs in PDGF mice between each group (2, 3, 4 months)	40
REFERENCE	44
ABBREVIATION	51
ACKNOWLEDGEMENT	54

SUMMARY

The main pathological feature of Parkinson's disease (PD) is the formation of Lewy bodies in the substantia nigra (SN). Alpha synuclein (α -syn) misfolds and aggregates into insoluble amorphous or fibrillar amyloid-like assemblies, which is the core component of Lewy bodies. α -syn aggregation is implicated in altered synaptic function and ultimately results in synaptic loss and even neuronal death. MicroRNAs (miRNAs) are defined as crucial part of our genome and are involved in various cellular processes, such as neuronal cell death, synaptic dysfunction and inflammatory response. Recently, a differential expression of miRNAs has been found in PD patients' brains. However, the pathophysiological relevance of these findings is still not understood, and require to be analyzed in animal models of PD. In order to shed light on the role of miRNAs for synaptic loss in PD, miRNA sequencing was performed in PDGF-hum- α syn transgenic mouse that show synaptic loss already at 3 months of age. The differential expression of miRNAs was studied prior to the loss of synapses at 2 months of age and in an age when spine loss has been documented at 3 and 4 months of age. Very few miRNAs changes were observed between 3 and 4 months old PDGF mice. However, when 3- and 4-month-old PDGF mice were compared to 2-month-old mice, several differential expressed mi-RNAs were observed including mir-184-3p, mir-182-5p, mir-34c-5p and mir-200b-3p. These miRNAs changes might contribute to early synaptic loss that occurs between the 2 and 3 months in young PDGF mice. Collectively, this dissertation shows for the first time a correlation of the expression of miRNAs mir-184-3p, mir-182-5p, mir-34c-5p and mir-200b-3p with dendritic spine loss in a PD mouse model.

ZUSAMMENFASSUNG

Das pathologische Hauptmerkmal der Parkinson-Krankheit (PD) ist der Nachweis von Lewy-Körpern in der Substantia nigra (SN). Alpha-Synuclein (α -syn) faltet sich fehlerhaft und aggregiert zu unlöslichen amorphen oder fibrillären Amyloid-ähnlichen Aggregaten, welche der Kernbestandteil der Lewy-Körper und Lewy Neuriten sind. Darüber hinaus geht man davon aus, dass die α -syn-Aggregation die synaptische Funktion beeinträchtigt und zu einem Verlust von Synapsen und dem Untergang von Nervenzellen führt. MicroRNAs (miRNAs) sind definiert als wesentlicher Bestandteil unseres Genoms und sind an verschiedenen zellulären Prozessen beteiligt, wie z. B. dem Absterben von Nervenzellen, synaptischen Dysfunktionen und Entzündungsreaktionen. Vor kurzem wurde eine differentielle Expression von miRNAs im Gehirn von PD-Patienten beschrieben. Allerdings ist die pathophysiologische Relevanz dieser Befunde noch nicht verstanden und erfordert die Untersuchung von Tiermodellen der PD. Um die Rolle von miRNAs bei dem Verlust von Synapsen in PD aufzuklären, wurde miRNA-Sequenzierung bei transgenen PDGF-hum- α syn-Mäusen durchgeführt, welche bereits im Alter von 3 Monaten einen Verlust der Synapsen aufwiesen. Die differentielle Expression von miRNAs wurde vor dem Verlust von Synapsen im Alter von 2 Monaten untersucht, sowie in einem Alter, in dem ein Verlust der Dornenfortsätze im Alter von 3 und 4 Monaten dokumentiert wurde. Es wurden sehr wenige Veränderungen der miRNAs zwischen 3 und 4 Monate alten PDGF-Mäusen beobachtet. Jedoch wurden beim Vergleich von 3 und 4 Monate alten PDGF-Mäusen mit 2 Monate alten Mäusen mehrere differentiel exprimierte miRNAs gefunden, einschließlich mir-184-3p, mir-182-5p, mir-34c-5p und mir-200b-3p. Diese

Veränderungen der miRNAs könnten zu einem frühen synaptischen Verlust beitragen, welcher zwischen 2 und 3 Monaten bei jungen PDGF-Mäusen auftritt.

Zusammenfassend zeigt diese Dissertation zum ersten Mal eine Korrelation der Expression der miRNAs mir-184-3p, mir-182-5p, mir-34c-5p und mir-200b-3p mit dem Verlust der dendritischen Dornenfortsätze in einem PD-Mausmodell.

INTRODUCTION

1. Parkinson's disease

PD is the most common neurodegenerative movement disorder worldwide. Over 7 million people are affected (Sherer, 2011). The main features of PD are bradykinesia, impaired posture and balance, muscle rigidity and tremor (Aron et al., 2010). Pathological hallmarks of PD are the progressive loss of dopaminergic (DA) neurons in the substantia nigra pars compacta (SNpc), the formation of Lewy bodies by the accumulation of alpha-synuclein (α -syn) (Leggio et al., 2017). The underlying mechanisms of PD have been partially illustrated in recent years. It was demonstrated that a mutation in VPS35 cause to late-onset PD (Zimprich et al., 2011). Mutations in leucine rich repeat kinase 2 (LRRK2) have been confirmed to result in familial PD (Liu et al., 2012). Furthermore, microRNAs (miRNAs) are also considered to be involved in the progression of PD.

2. Cognition impairment of Parkinson's disease

Cognitive impairment, including dementia (Parkinson's disease dementia, PDD), is a common characteristic in PD patients. In PDD, the onset of dementia is usually several years after the PD diagnosis. Propagation of α -syn aggregates to the neocortical regions according to the Braak-PD staging (Figure 1) is the main substrate of cognitive decline in PDD (Emre et al., 2007).

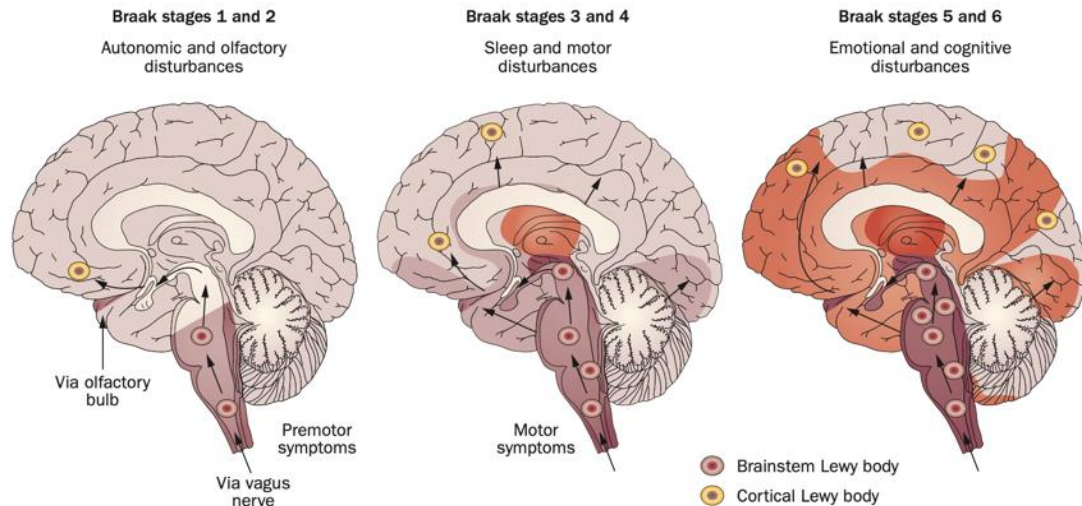


Fig. 1: The Braak staging system of PD

There are 6 stages by pathological classification in PD. The α -syn pathology spreads from the olfactory bulb and medulla oblongata, pass the limbic system to the neocortex. The red shading displays the pattern of pathology. (From Doty, 2012)

It has widely been accepted that memory formation is linked to synaptic plasticity, which is the alters in the strength of the synaptic connections between neurons. Synaptic dysregulation in the hippocampus and association cortices are considered as an early characteristic and related to the severity of cognitive decline in Alzheimer disease (AD) (DeKosky et al., 1996). It was also reported that the PD patients carried the mutation of glucocerebrosidase gene show lower nigrostriatal dopamine transporter density and reduced synaptic activity in parietal and posterior cortices (Cilia et al.,2016).

2. Alpha-synuclein

Alpha-synuclein (α -syn), a small (14 kDa) cytosolic protein, is the main component of Lewy bodies. It contains 3 sections: an amphipathic N-terminal domain which interacts with lipid membranes, an acidic C terminal region function on the suppression of aggregation, and a central hydrophobic core related to protein aggregation (Snead et al., 2014).

Under physiological conditions, α -syn, a natively unfolded monomer in the cytoplasm, is involved in the clustering of synaptic vesicles (Burré et al., 2010; Maroteaux et al., 1988), whereas under pathological conditions, α -syn is misfolded into pathogenic species (dimers, trimers and oligomers) which ultimately hamper synaptic function and cause neuronal death (Calo et al., 2016) (Figure 2).

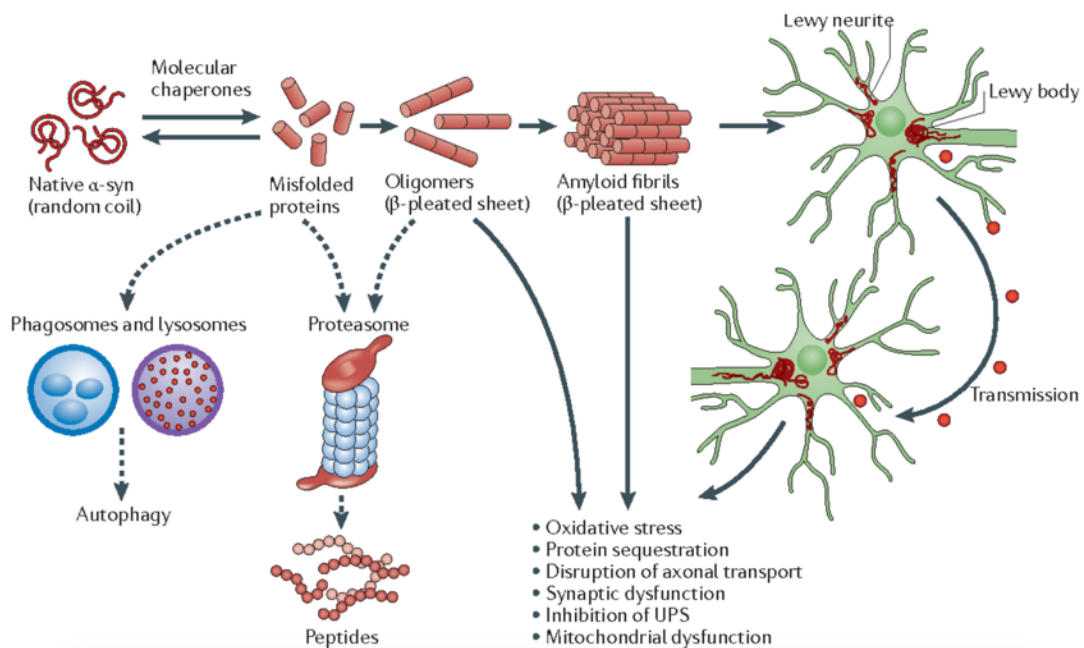


Fig. 2: Hypothetical model of α -syn toxicity and spread of pathology in PD

Misfolded proteins aggregate into higher-order structures which contains protofibrils, other intermediates and amyloid fibrils, they are the pathological foundational composition of α -syn, and eventually form Lewy bodies. Chaperones, ubiquitin proteasomes and phagosome-lysosome systems, also called normal quality-control systems, function on avoiding protein misfolding or removing misfolded proteins, however, oligomeric species of α -syn could cause to the dysfunction of this system. (Kingwell, 2017)

Recent data confirm that the progression of PD may be implicated to the cell-to-cell spread of pathological structures of α -syn. The transmission of α -syn is considered to have various toxic consequences, including oxidative stress, protein sequestration, disruption of axonal transport, synaptic dysfunction, inhibition of UPS and mitochondrial dysfunction.

In the brain, α -syn is found mainly in presynaptic terminals of neurons. Presynaptic terminals release neurotransmitters from synaptic vesicles. Normal brain functions via the release of neurotransmitters transfers signals between neurons. Although the function of α -syn is not well understood, it was confirmed that α -syn plays an important role in maintaining a sufficient supply of synaptic vesicles in presynaptic terminals. It may benefit to mediate the dopaminergic release, which is a neurotransmitter and important for the controlling of starting or stopping movements.

3. MicroRNAs

MicroRNAs (Figure 3) were first described in 1993 (Lee et al., 1993). They are a class of 21-25 nucleotides (nt) long, non-coding and single-stranded RNA that regulate the expression of genes (Kabiri Rad et al., 2018; Boese et al., 2016; Doeppner et al., 2013; Chédotal, 2011). The miRNAs are demonstrated to be implicated in various stages of growth, development, and differentiation of the cells (Jan Christoph Koch et al., 2012), and enriched and active in the brain (Meza-Sosa et al., 2014).

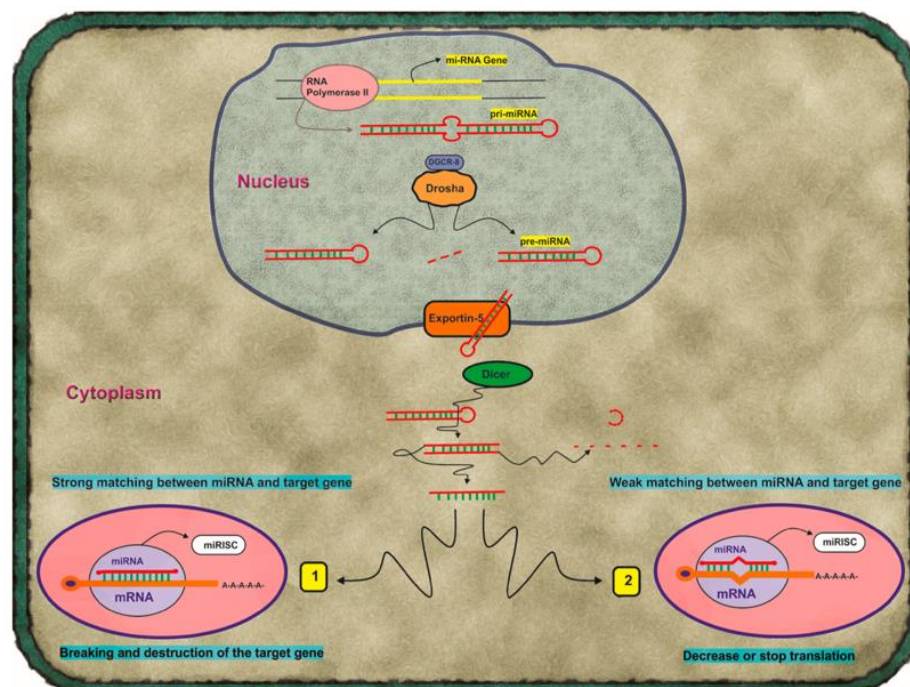


Fig. 3: miRNA biogenesis pathway and function

First, a primary transcript (pri-miRNA) is generated from the miRNA gene by the RNA polymerase II. Then, Drosha complex and DiGeorge syndrome chromosomal region-8 cleaved the pri-miRNA into precursor miRNAs, which is 70 nucleotides stem-loop transcripts. Then, pre-miRNA is transported to the cytoplasm by exportin 5. After that, double-strand miRNA is generated by the cleavage of Endoribonuclease III Dicer. After denaturing by helicase, mature miRNA is generated from one single-strand, another strand degrades. At last, the mature miRNA interacts with the RNA-induced silencing complex in two different pathways, which results in the modulation of the mRNA gene expression. (Khodadadian et al., 2018)

The role of miRNAs in PD pathogenesis is still unclear, however a few studies in PD patients and animal models were performed, in which miRNAs were identified as powerful regulators of physiological and pathological cellular processes (Sayed et al., 2011). The increase of mir-184 was confirmed to attenuated pathogenic leucine-rich repeat kinase 2 (LRRK2, its mutations were proofed to result in PD) effects in *Drosophila* (Gehrke et al., 2010). Mir-7 was reported to repress α -syn expression, and to facilitate the degradation of pre-formed fibrils of α -syn (Choi et al., 2018). Mir-132 was considered to involve in maintaining of synaptic plasticity for memory function (Nadim et al., 2017), the repression of mir-132 was demonstrated to affect the maturation of dendritic spines *in vivo* (Mellios, 2011). More and more miRNAs are considered to play an important role in PD pathogenesis (Lewis, 2014; Kim et al., 2007). The study of the role of miRNAs in PD is therefore a novel approach to understanding PD pathogenesis.

4. PD mouse models

Some studies demonstrated that the differential expression of miRNAs exist in PD patients' brain (Hoss et al., 2016), implying that these miRNAs play a role in PD pathogenesis. However, to do functional research on miRNAs in humans is difficult and animal models are useful tools in PD translational research.

Numerous lines of mice overexpressing normal α -syn or α -syn with pathogenic mutations (e.g. A53T, A30P) have been generated using distinct promoters (e.g. Thy-1, PDGF- β) and transgenes (Fernagut et al., 2004). The main advantage of α -syn models is that α -syn positive inclusions could be replicated, although the typical Lewy bodies in human PD is not found in murine (Maries et al., 2003). Reduced olfaction, autonomic dysfunction, α -syn accumulation and motor deficits are the features of mice with overexpressing wild-type human α -syn, however, the model is lack of nigrostriatal neurodegeneration (Rockenstein et al., 2002; Fleming et al., 2004; Chesselet et al., 2008; Fleming et al., 2008).

PDGF-hum- α syn transgenic mouse model was used for the study in this dissertation. These mice overexpress human α -syn under the control of the human PDGF- β promoter. α -syn is strongest expressed in the neocortex, hippocampus, olfactory bulb, and limbic system, and accumulated starting at 3 months of age (Amschl et al., 2013; Masliah et al., 2000). It was reported that synaptic loss starts from 3 months of age in the neocortex of PDGF mice (Blumenstock et al., 2017).

5. Aim of the study

In order to identify miRNAs changes directly and possibly causally related to synaptic plasticity in the young PDGF mice, miRNA sequencing was performed in 2-, 3- and 4-months old animals. MiRNA sequencing was performed applying next-generation sequencing to sequence all miRNAs in a given sample in order to discover miRNAs changes that coincide with the loss of synapses.

MATERIAL AND METHODS

1. Animals

PDGF-hum- α -syn mice were supported from QPS Austria Neuropharmacology (Grambach, Austria) and bred on a C57Bl/6 background. All mice were kept under pathogen-free conditions in the animal facility of the ZNP (Center for Neuropathology and Prion Research) of the LMU (Ludwig-Maximilians-University of Munich). All mice were housed in groups (maximum of 5 mice per cage) with food and water provided ad libitum and kept on a 12h light/ dark cycle, the room temperature maintained at $21 \pm 1^\circ\text{C}$. The body weight and health state were checked every day. All experiments were approved by the Bavarian government (Az. 55.2-1-54-2532-163-13) and performed according to the animal protection law. The mice used in these experiments are listed in Table 1.

Table 1: list of mice line

ID No.	PDGF	Age (month)	Gender*	ID No.	PDGF	Age (month)	Gender	ID No.	PDGF	Age (month)	Gender
734	-	2	M	658	-	3	F	653	-	4	F
733	-	2	M	657	-	3	F	648	-	4	F
717	-	2	F	661	-	3	M	652	-	4	F
719	-	2	M	663	-	3	M	649	-	4	M
737	-	2	F	660	+	3	M	676	+	4	M
716	-	2	F	656	+	3	F	671	+	4	F
713	+	2	F	662	+	3	M	651	+	4	F
721	+	2	M	654	+	3	F	647	+	4	F
714	+	2	F	659	+	3	M	674	+	4	M
715	+	2	F	655	+	3	F	675	+	4	M
718	+	2	M								
720	+	2	M								

* M and F represent male and female.

2. Genotyping

In order to determine the genotypes of all mice, polymerase chain reaction (PCR) was performed. The Invisorb® DNA Tissue HTS 96 Kit (Invitek molecular) was used for DNA extraction. In brief, 20mg mouse tissue was used to isolate DNA, it was incubated with 400 µl of Lysis Buffer G overnight at 52°C, then the mixture was centrifuged for 10 min at 1700 g. The supernatant was transferred into a new collection tube and mixed with 200 µl Binding Buffer A, then the mixture was centrifuged for 5 min at 1700 g. After discarding the supernatant, 550 µl Washing Buffer was added into the pellet, followed twice by 5 min centrifugation at 1700 g. Lastly, the DNA extraction was obtained after washing with 100 µl of prewarmed (52°C) Elution Buffer.

PCR was performed with the extracted DNA to identify the genotype of mice. The primer 209F (CTGGSSGSTATGCCTGTGGA) with 20 bp length and 50R (CATCAATGTATCTTATCATGTCTGGATTCT) with 29 bp length were used in this study. The reagents for PCR reaction was listed in Table 2, the PCR program was listed in Table 3. Then the PCR products were loaded on a 1.0% agarose gel, and analyzed by gel electrophoresis (120-195 V, 60-90 min). After that, post-staining was performed with SYBR® gold nucleic acid gel stain for 5 min. Finally, a photograph of the gel was taken under UV light source.

Table 2: PCR solution for genotyping

Items	Volume	Concentration
Onetaq hotstart quickload	12.5 µl	
209F	0.5 µl	10 µM
50R	0.5 µl	10 µM
Template DNA	1 µl	
Distilled water	10.5 µl	

Table 3: PCR program for genotyping

Step	Temperature (°C)	Time (s)
1	94	180
2	94	30
3	60	60
4	68	20
5	68	300
6	10	∞
Step 2-4: repeat for 27 times.		

3. Total RNA and small RNA isolation

Total RNA or small RNA was isolated by using a Qiagen® miRNeasy Micro Kit (No. 217084). In brief, 5 mg murine cortical tissue was thoroughly homogenized with 700 µl QIAzol Lysis Reagent in a collection tube by using a plastic pestle, then placed it at RT for 5 min. Next, the homogenate was incubated at RT for 2-3 min after mixing with 140 µl chloroform, followed by 12000 g centrifugation at 4°C for 15 min (Eppendorf, Centrifuge 5804R). Then, the total RNA isolation or small RNA isolation was correspondingly performed following the steps in **3.1** or **3.2**.

3.1 Total RNA isolation

The supernatant of homogenate was transferred to a new tube, vortexed for 10 sec after adding 525 µl of 100% ethanol (total volume: 900 µl). 700 µl of the mixture was pipetted into an RNeasy MinElute spin column in a 2 ml collection tube, followed by 8000 g centrifugation for 15 sec at room temperature (RT), then the flow-through was discarded (this step would be repeated with the remaining mixture). After that, 700 µl Buffer RWT was added into the column, followed by 8000 g centrifugation for 15 sec. After that, 500 µl of 80 % ethanol was pipetted into the column, followed by 8000 g centrifugation for 2 min. Then the flow-through was discarded. In order to dry the membrane of the column, centrifugation was performed for the column in a new tube

for 5 min at full speed, then the flow-through was discarded. Lastly, 14 µl of RNase-free water was added into the column in a new 1.5 ml tube, after centrifuging at full speed for 1 min, the total RNA was collected in the tube.

3.2 Small RNA isolation

The supernatant of homogenate was transferred to a new tube and mixed with 350 µl of 70 % ethanol. 700 µl of the mixture was pipetted into an RNeasy MinElute spin column in a 2 ml collection tube, followed by 8000 g centrifugation at RT for 15 sec, the flow-through containing the small RNA was kept. Then the flow-through was mixed with 450 µl of 100% ethanol, the total volume of the mixture was approximately 1150 µl. 700 µl of the mixture was pipetted into a new RNeasy MinElute spin column in a new 2 ml tube, followed by 8000 g centrifugation at RT for 15 sec, the flow-through was discarded (this step would be repeated with the remaining mixture). Next, 700 µl of Buffer RWT was pipetted to the column, then centrifuged the column at 8000 g for 15 sec, the column was kept. Then 500 µl of Buffer RPE was pipetted to the column followed by 8000 g centrifugation for 15 sec. After that, 500 µl of 80 % ethanol was added to the column, then centrifuged at 8000 g for 2 min, then the membrane of column was dried by 8000 g centrifugation for 5 min. Lastly, 14 µl RNase-free water was added into the column in a new tube, after centrifuging at 8000 g for 1 min, the small RNA was collected in the tube.

4. Concentration measurement of double strand DNA (ds DNA)

Qubit 3.0 Fluorometer (Invitrogen™, Q33216) and Qubit™ dsDNA HS Assay Kit (Thermo Fisher, Q32851) were used for concentration measurement of dsDNA. In brief, the working solution was prepared by diluting the dsDNA HS Reagent 1:200 in dsDNA HS Buffer. 190 µl of working solution and 10 µl of standard reagent 1 (or 2) were mixed in the tube used for standard 1 (or 2). Then 199 µl of working solution and 1 µl of a

sample was mixed in a new tube. After incubation at RT for 2 min, the standard tubes were inserted into the sample chamber of Qubit 3.0 Fluorometer, and the concentration of the standards was read by running dsDNA system. Followed by running with sample tubes, the concentration was read out and saved as documentation.

5. Western blot

20 mg of murine cortical tissue was used for western blot analysis to identify the expression of α -syn protein in PDGF mice. 200 μ l of homogenate buffer (the formulation was listed in Table 4) was mixed with the tissue in a 1.5 ml collection tube, then the mixture was homogenized by using a plastic homogenizer on ice. After that, the total protein in each sample was quantitated by using the Bicinchoninic Acid protein assay (BCA protein assay, Smith et al., 1985). 20 and 50 μ g of protein for each sample was added to 2 lanes of 12.5% SDS-PAGE gel (the formulation was listed in Table 5), respectively. Then the protein migration was driven by electrophoresis in running buffer (the formulation was listed in Table 6) at 80 V for 20 min, followed by electrophoresis at 120 V for 40 min. Next, the protein was transferred to the PVDF membrane by using semi dry blotting for 2 h (the formulation of transfer buffer was listed in Table 7). This was followed by membrane incubation in PBS with 4% PFA and 0.01% Glutaraldehyde for 30 min at RT and then the membrane was washed with 1 \times TBST for 5 \times 4 min. Next, the membrane was placed in Ponceau dye (0.2% Ponceau S, 3% acetic acid) for 5 min to stain for total protein. After washing the membrane with deionized water to remove the excessive Ponceau dye, the membrane with protein bands was scanned for saving as documentation. Following incubation in 5% TBST-milk for 1 h, the membrane was placed in 50 ml of 5% TBST-milk including 5 μ l of α -syn antibody 4B12 (ThermoFisher scientific, #MA1-90346) at 4°C overnight. Then the membrane was washed with 1 \times TBST for 3 \times 5 min and incubated, followed by incubation in 25 ml of

5% TBST-milk included 5 μ l of anti-Mouse-HRP secondary antibody (Cell Signaling Technology, #7076) at RT for 1 h. Then the membrane was washed by 1 \times TBST for 3 \times 5 min, followed by incubation with 2 ml of ECL solution at RT for 2-3 min. Finally, the protein bands on the membrane were detected by using Chemostar ECL and Fluorescence Imager (Intas science imaging).

Table 4: Formulation of homogenate buffer

Item	Volume
PMSF	10 μ l
NEM	10 μ l
miniComplete EDTA-free protease inhibitor (Roche)	1 tablette
NP-40	100 μ l
TBS (50 mM Tris pH 7.5, 175 mM NaCl, 1 mM MgCl ₂)	9.88 ml

Table 5: Formulation of 12.5% SDS-PAGE gel

Stacking gel		Separation gel	
Item	Volume	Item	Volume
1.5 M Tris-HCl pH 8.8 (0.4% SDS)	1.7 ml	0.5 M Tris-HCl pH 6.8 (0.4% SDS)	3.75 ml
Deionized water	4.9 ml	Deionized water	6.35 ml
30% Acrylamide/Bis-acrylamide (29:1)	925 μ l	30% Acrylamide/Bis-acrylamide (29:1)	4.75 ml
Temed	7.5 μ l	Temed	12.5 μ l
10% APS	75 μ l	10% APS	125 μ l

Table 6: Formulation of 10 \times running buffer

Item	Volume
Tris base	30 g
Glycine	144 g
SDS	10 g
Deionized water	1000 ml

Table 7: Formulation of transfer buffer

Item	Volume
Tris base	7.58 g
Glycine	36 g
Methanol	500 ml
Deionized water	2500 ml

6. MiRNA sequencing

The miRNA sequencing (Figure 4) was performed to identify the miRNAs abundance and differential expression by using Illumina® NextSeq 550 System.

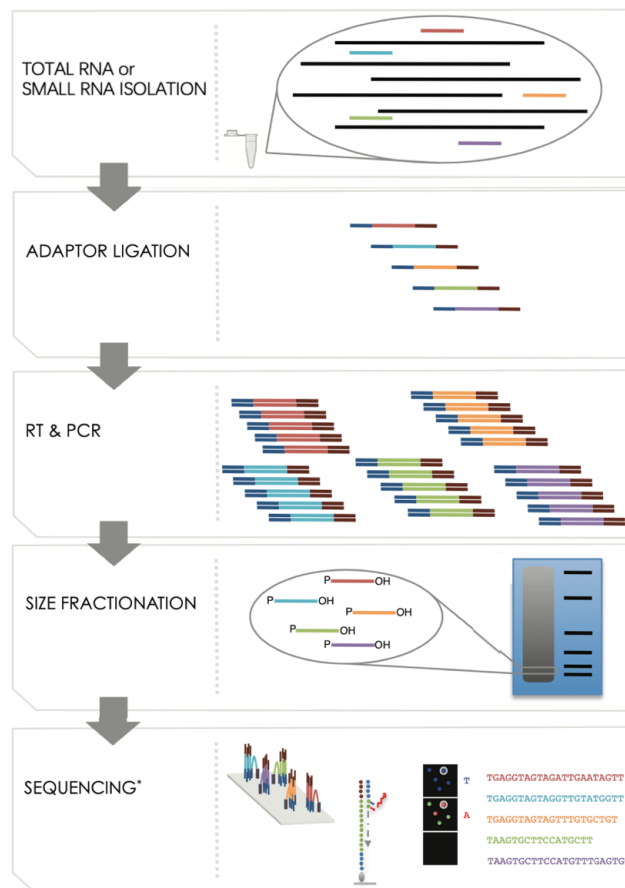


Fig. 4: The workflow of miRNA sequencing

Firstly, the total RNA or small RNA isolated from a sample is used for miRNA sequencing. Secondly, the adaptors are ligated to total RNA or small RNA. Thirdly, reverse transcription and amplification of the products are performed to get the cDNA. Next, a gel purification to fractionate the cDNA fragments with specific sizes (145-160 bp) which corresponded to miRNAs length (22-25 nt) plus adaptors has to be performed. Lastly, miRNA sequencing is performed with a sequencer.

6.1 Adapters Ligation

5 μ l of a sample including 50 ng of small RNA was incubated with 1 μ l of RNA 3' Adaptor at 70°C for 2 min. Then the sample was incubated with 2 μ l of Ligation Buffer, 1 μ l of RNase Inhibitor and 1 μ l of T4 RNA Ligase 2 (Deletion Mutant, Biozym, 138031) at 28°C for 1 h. After that, the sample was incubated with 1 μ l of Stop Solution at 28°C for 15 min, the products named RNA 3' Adaptor mixture. At the meanwhile, a new PCR tube with 1 μ l of RNA 5' Adaptor was incubated at 70°C for 2 min, then the RNA 5' Adaptor together with 1 μ l of ATP and 1 μ l of T4 RNA Ligase were added to the RNA 3' Adaptor mixture and the mixture was incubated at 28°C for 1 h. The total volume of the mixture named adapter-ligated RNA library was 14 μ l.


6.2 cDNA template preparation (Reverse Transcription and PCR)

6 μ l of the adapter-ligated RNA library was incubated with 1 μ l of RNA Reverse Transcription Primer in a new tube at 70°C for 2 min. Then the products were incubated with 2 μ l of First Strand Buffer, 0.5 μ l of dNTP Mix (12.5mM), 1 μ l of DTT, 1 μ l of RNase Inhibitor and 1 μ l of SuperScript II Reverse Transcriptase (Invitrogen™, 18064014) at 50°C for 1 h. After that, 8.5 μ l of Ultrapure water, 25 μ l of PCR Mix, 2 μ l of RNA PCR Primer and 2 μ l of Index were added to the sample and underwent PCR with the program listed in Table 8.

Table 8: PCR program for miRNA sequencing

Step	Temperature (°C)	Time (s)
1	98	30
2	98	10
3	60	30
4	72	15
5	72	600
6	4	∞
Step 2-4: repeat for 11 times.		

6.3 Quality control of the samples

The size and concentration of cDNA was checked with a High Sensitivity DNA chip (Agilent, 5067-4626) by using Agilent Bioanalyzer 2100. In brief, 15 μ l of High Sensitivity DNA dye concentrate was mixed with 300 μ l of High Sensitivity DNA gel matrix after incubation at RT for 30 min, followed by 2240 g centrifugation for 15 min. Then a High Sensitivity DNA chip was placed on the priming station. 9 μ l of gel-dye was added in the well which was marked with , followed by closing the chip priming station, and pressing the plunger from 1 ml to the bottom until it was held by clip. 1 min later, the clip was released. Next, 9 μ l of gel-dye was added in the wells which was marked with G, 5 μ l of marker was added in all sample and ladder wells. Then 1 μ l of ladder was pipetted in the ladder well, and 1 μ l of each sample was added in the corresponding sample well. After 2400 rpm vortexing for 1 min, the chip was placed on the Agilent bioanalyzer 2100. The following figure 5 shows typical results from human brain total RNA.

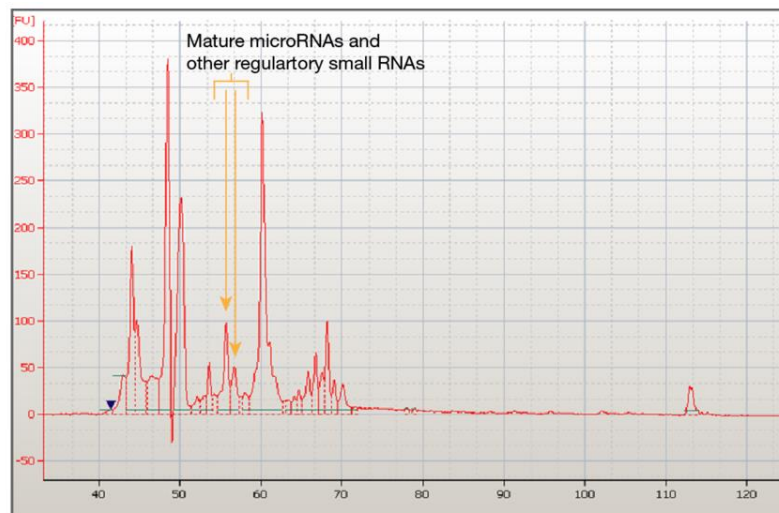


Fig. 5: Sample trace of amplicons on a High Sensitivity DNA Chip

The x axis shows the timeline (also can be changed to size scale), the y axis shows fluorescence absorption intensity. The first and last peaks were the lower and upper marker peaks. The other peaks represent the cDNA fragments with different sizes, respectively. The yellow arrows point out the mature miRNAs and other regulatory small RNAs.

6.4 Size Fractionation (gel purification of cDNA)

Since the size of miRNAs was 22-25 nt, the length of corresponding cDNA would be 145-160 bp (the length of adaptors was around 130 nt), thus the cDNA fragments with 145-160 bp length had to be purified.

Firstly, all the samples were pooled together in equimolar amounts based on the concentration measured by Qubit™. Secondly, the gel purification was performed with 8% native PAGE gel (Figure 6, Illumina Document #15004197 v02). 2 µl of High-Resolution Ladder was mixed with 2 µl DNA loading dye, then the mixture was loaded to the first and last lanes of gel in equal amounts as size ladders. Then 2 µl of Custom RNA Ladder was mixed with 2 µl DNA loading dye, the mixture was averagely loaded to the lanes closed to the High-Resolution Ladder as the controls. After that, 50 µl of the sample was mixed with 10 µl DNA loading dye, then the mixture was averagely loaded to 2 lanes between the Custom RNA Ladders. After that, DNA migration was driven by 80 V for 120 min until the blue front dye left the gel.

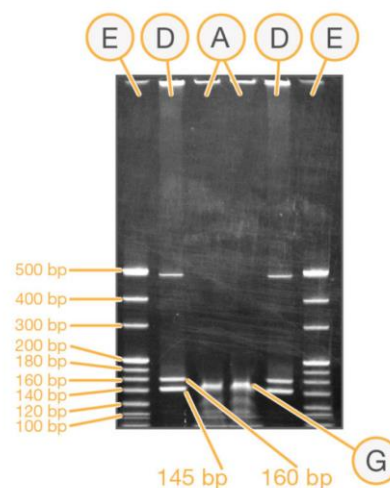


Fig. 6: Gel purification for the cDNA template of miRNA

Ⓐ shows the lanes loaded with the sample. Ⓒ shows the bands of miRNAs fragments between 145 and 160 bp. Ⓓ presents the controls named Custom RNA Ladder. Ⓔ presents the size ladder named High-Resolution Ladder.

Thirdly, the gel was placed in 100 ml running buffer with 10 μ l SYBR™ Gold Nucleic Acid Gel Stain (Invitrogen™, S11494) for 5 min, then the DNA bands could be seen under the blue light (Invitrogen™ E-Gel™ iBase™ and E-Gel™ Safe Imager™ Combo Kit, 10001123). The bands of the sample size between 145 and 160 bp were cut down and placed into a 0.5 ml gel breaker tube within a 2 ml collection tube, followed by 20000 g centrifugation for 2 min to collect the gel debris. Then 200 μ l of ultrapure water was added to the gel debris, followed by 500 rpm shaking for at least 2 h by using a Thermomixer to elute the DNA. Next, the debris was transferred to a 5 μ m filter in a 2 ml collection tube, followed by 600 g centrifugation for 10 sec, the flow-through was collected for further miRNA sequencing. The quality of the sample was checked with Bioanalyzer analysis, the concentration was also measured by using Qubit and normalized to 4 nM by using Resuspension Buffer (RSB) (Illumina, FC-110-3002). The formulation of converting ng/ μ l to nM for dsDNA is as follows:

$$\frac{\text{Concentration in ng}/\mu\text{l} \times 10^6}{660 \text{ g/mol} \times \text{average library size in bp}} = \text{Concentration in nM}$$

6.5 Denature and dilute the sample

5 μ l of the sample (4 nM) was mixed with 5 μ l of 0.2 N NaOH, followed by 280 g centrifugation for 1 min, incubated it at RT for 5 min. Then 5 μ l of Tris-HCl (200 mM, pH 7) was added to the sample, followed by 280 g centrifugation for 1 min. After that, 985 μ l of Hybridization buffer was added to the sample, followed by 280 g centrifugation for 1 min, thus the sample was diluted to 20 pM. Next, 117 μ l of the sample (20 pM) was mixed with 1183 μ l of Hybridization buffer, in order to dilute the sample to 1.8 pM, the total volume of was 1.3 ml.

6.6 Sequencing on the Illumina platform

1.3 ml of the sample (1.8 pM) was loaded on the NextSeq 500/550 High Output Flow Cell Cartridge (75 Cycles. Illumina, No. 20024906), then the sequencing was performed on NextSeq 550 platform (Illumina, SY-415-1002).

7. Data processing

For miRNA sequencing data analysis, the Galaxy bioinformatics analysis platform was used for the assessment of the raw reads, the alignment of reads to the genome and the quantification of gene expression. Reads were counted per sample using the Rsubread package (Chen et al., 2016) and the miRNA annotation database version 22 from miRbase (<http://www.mirbase.org/>). EdgeR package (Robinson et al., 2010) was used for differential expression analysis of miRNAs. P-value was adjusted using q-value. And q-value < 0.1 was set as the threshold for significantly differential expression by default.

RESULTS

Based on that accumulation of α -syn resulted in the decline of cortical spine density in young adult PDGF mice starting from 3 months of age (Blumenstock et al., 2017), a hypothesis came out that several miRNAs may mediate synaptic loss in young PDGF mice. In order to analyze the expression of miRNAs, miRNA sequencing was performed in cortical tissue of PDGF mice and controls at different time points (2-, 3- and 4- months). Information of mice age and gender that have been studied is listed in Table 9.

Table 9. Mice used in this study

ID No.	PDGF	Age (month)	Gender*	ID No.	PDGF	Age (month)	Gender	ID No.	PDGF	Age (month)	Gender
734	-	2	M	658	-	3	F	653	-	4	F
733	-	2	M	657	-	3	F	648	-	4	F
717	-	2	F	661	-	3	M	652	-	4	F
719	-	2	M	663	-	3	M	649	-	4	M
737	-	2	F	*660	+	3	M	*676	+	4	M
716	-	2	F	656	+	3	F	671	+	4	F
713	+	2	F	662	+	3	M	651	+	4	F
721	+	2	M	654	+	3	F	647	+	4	F
*714	+	2	F	659	+	3	M	674	+	4	M
715	+	2	F	655	+	3	F	675	+	4	M
718	+	2	M								
720	+	2	M								

* M and F represent male and female. * ID No. 714 mouse was excluded from further analysis (see Chapter 2.2.1 of Results). * ID No. 660 and 676 mice were also excluded from further analysis since α -syn was not expressed in these PDGF mice (see Chapter 1 of Results).

1. α -syn expression identification in PDGF mice

In all PDGF mice, a western blot analysis was performed in order to confirm the expression of the human α -syn transgene. An α -syn monoclonal antibody (4B12) was used as primary antibody, and anti-mouse IgG, HRP-linked antibody was used as secondary antibody to bind to the primary antibody. A band of 15-25 kDa was detected

which confirmed the expression of the human α -syn transgene in these mice (Figure 7A-C).

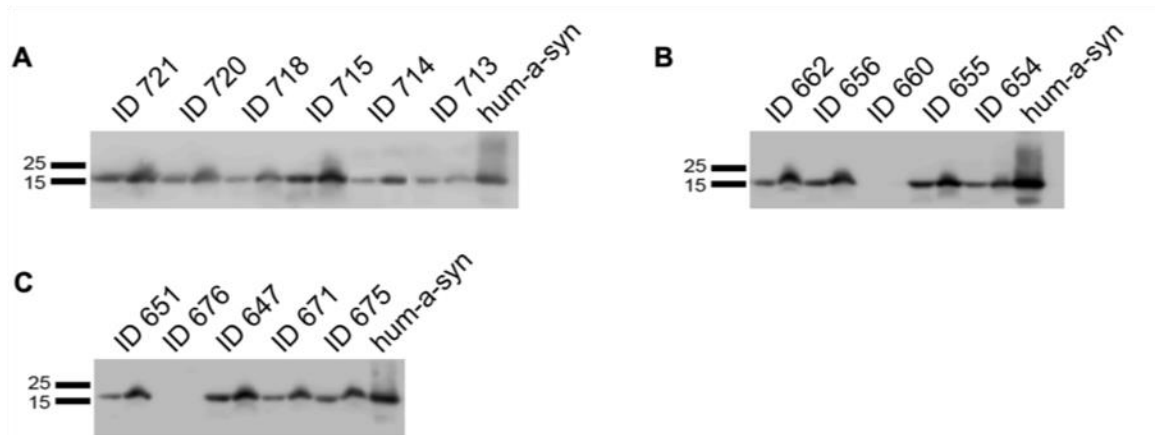


Fig. 7: Expression of the human α -syn transgene in PDGF mice

12.5% SDS-PAGE gel was used for western blot analysis. Each sample was loaded on 2 lanes with the total protein amount of 20 and 50 μ g respectively. Cortical tissue from PDGF mice at the age of 2 months (A), 3 months (B) and 4 months (C) were analyzed for the expression of the human α -syn transgene. The bands which molecular weight between 15 and 25 kDa represent α -syn protein. PDGF mice number: n=6 (2 months), n=5 (3 months), n=5 (4 months).

The results showed that 1 out of 5 3-month-old PDGF mice did not express the α -syn transgene, and also 1 out of 5 4-month-old PDGF mice did not express it. These 2 mice (ID No. 676 and 660) were excluded from further analysis.

2. Analysis of miRNA expression in PDGF mice

In order to observe miRNAs changes at different time points in PDGF mice, miRNA sequencing was performed. Firstly, small RNAs (length less than 200 nt) were isolated from each murine cortical tissue, including miRNAs, which are between 17 and 25 nt of length. Secondly, two adaptors (total length around 130 nt, including indexes, used for differentiating each sample) were ligated to the 5'- and 3'- termini of small RNAs, respectively. Then the products were transcribed into cDNA. Since miRNAs were the analytical targets in this study, the cDNA fragments length between 140 and 160 bp represented miRNAs transcription results and were purified from all cDNA fragments.

Finally, all the samples were mixed together in equimolar amounts and loaded for next generation sequencing.

2.1 Quality control of cDNA fragments for each sample

Before mixing all the samples together, the quality of each sample had to be determined. In order to determine the content of cDNA fragments length between 140 and 160 bp, an analysis which measured precise size and concentration of all dsDNA fragments was performed by using the Agilent Bioanalyzer, High Sensitivity DNA kit. The detection of fragments with 140-160 bp length implied that the quality of this sample was good. Figure 8 showed an exemplary analysis with cDNA for a 2-month-old mouse.

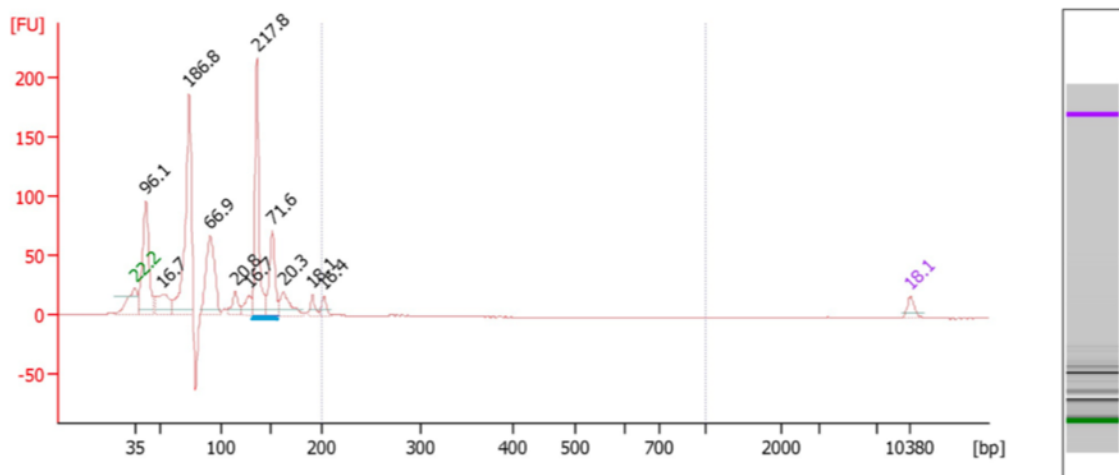


Fig. 8: Quality identification of cDNA fragments

The x axis represents size of fragments; the y axis displays fluorescence absorption intensity. The first and last peaks (is green and purple) are the lower and upper marker peaks. The other peaks represent the cDNA fragments with different sizes, respectively. The blue line points out the location of fragments with size between 140 and 160 bp.

The quality control was performed for all samples in this study, the results showed fragments of 140-160 bp length in all samples, therefore, the quality of all samples (2-, 3- and 4-month-old mice) was good and could be used for miRNA sequencing.

2.2 Data analysis after miRNA sequencing

In order to observe miRNAs expression level, sequencing was performed by using the NextSeq 500™ system of Illumina. The sequencing yielded a total of 3.5 Giga base pairs (Gbp) of raw data for all samples. Quality scores was used to check the probability of sequencing errors, Q30 represents an error rate of 0.1%, with an accuracy of 99.9%. It showed that 97.1% of data was identified to score higher than Q30, therefore, this data was considered to have good quality (Figure 9).

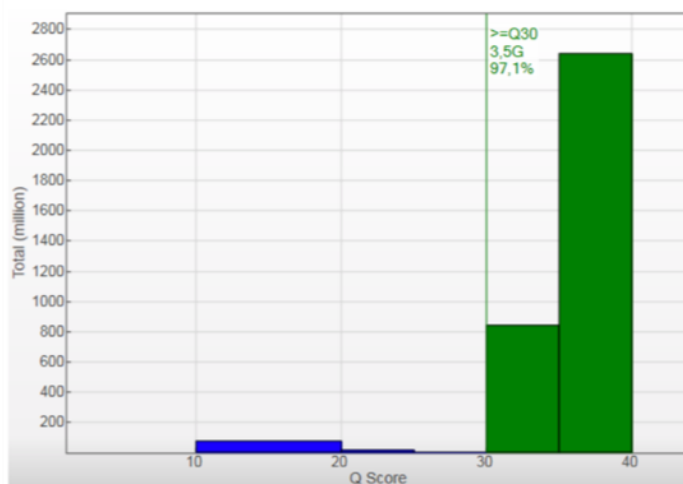


Fig. 9: Quality identification of miRNA sequencing datasets

The x axis represents Q scores; the y axis represents the yield of data (million base pairs). Green columns represent data with Q scores higher than 30. Blue columns indicate data with Q Scores lower than 30.

2.2.1 Prediction of overall similarity and difference between each sample

Galaxy Bioinformatics platform was used to analyze the data (<https://usegalaxy.org/>).

The samples could be distinguished based on the unique indexes for each sample. In order to visualize genetic distance and relatedness between each sample, a principal component analysis (PCA) was performed by using EdgeR package. PCA is a statistical technique which can be used to reduce the dimensions of a dataset. The number of variables retained in a PCA was determined by a method of scree test (Cattell, 1966). The bar graph showed the proportion of variability explained per

principal component (Figure 10A). PCA plot often contains the first two components, as these describe the largest variability (Figure 10B).

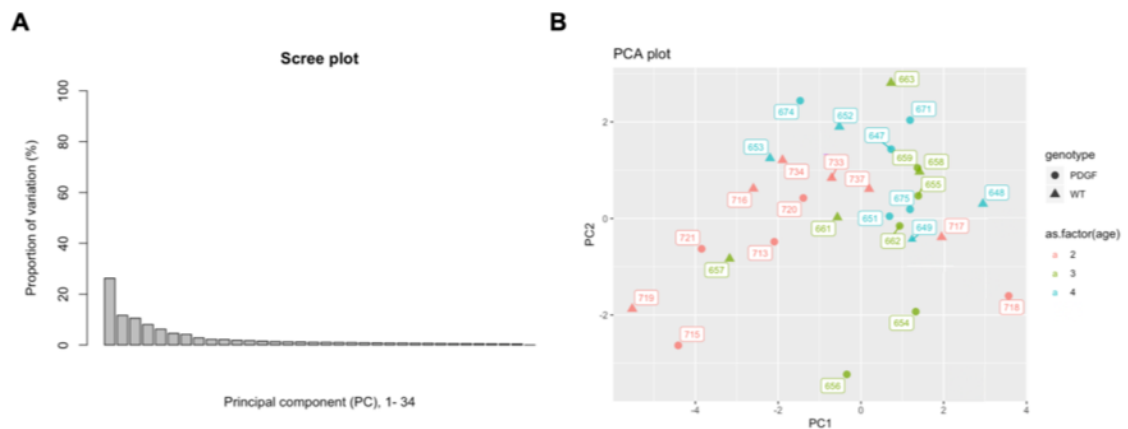


Fig. 10: Similarity prediction for each sample

(A) Screen plot gives the proportion of all PCs analysed. The x axis represents 34 of PCs, the y axis represents proportion of variation, the PCs are ordered in a decreasing ratio. (B) PCA plot displays the statistical distance between each sample. The x axis represents PC1 resulted from scree plot, the y axis represents PC2 resulted from scree plot. Each dot represents individual sample among 2-, 3- and 4-month-old mice and is distinguished by different colors and shapes.

The dots which represent 3- and 4-month-old PDGF mice were partially clustered. However, the dots which represent 2-month-old PDGF mice showed relatively more distance to the dots of 3- and 4-month-old PDGF mice. The results implied that 3- and 4-month-old PDGF groups are similar to some extent. One 2-month-old PDGF mouse (ID No.714) was excluded from further analysis to avoid deviation, since it was too far from the other sample dots (not shown on the PCA plot).

2.2.2 Differential expression of miRNAs in PDGF mice at different time points

In order to observe the differential expression of miRNAs in PDGF mice, the comparison analysis was performed with the EdgeR package.

2.2.2.1 General assessment of miRNAs' differential expression between 2-month-old mice and the other PDGF mice

Based on the finding that dendritic spine loss was detectable at the age of 3 months but not at 2 months of age in PDGF mice (Bumenstock et al., 2017), we ask the question if miRNAs expression change in PDGF mice between 2- and 3-month of age. Thus, a comparative analysis between PDGF mice older than 2 months (3- and 4-months old) and PDGF plus controls in 2-month-old was performed. The results revealed that 4 out of 1966 miRNAs (mir-184-3p, mir-182-5p, mir-34c-5p and mir-200b-3p) were significantly different in 3- and 4-month-old PDGF mice compared to 2-month-old mice (PDGF and controls) (FDR < 0.1, Figure 11A, 11B).

A

	gene	logFC.genotype PDGF.age3	logFC.genotype PDGF.age4	logCPM	F	FDR
1	mmu-miR-184-3p	-0.3190	1.9469	5.3925	18.5927661212016	0.00000001
2	mmu-miR-182-5p	-1.4316	-0.4262	9.2110	17.6365438560818	0.00000002
3	mmu-miR-34c-5p	0.5916	-0.3206	9.4986	9.57629878708313	0.00167955
4	mmu-miR-200b-3p	0.6148	0.6949	6.4211	9.01993832106281	0.00282065
5	mmu-miR-21a-5p	0.3147	-0.4426	11.3328	5.51136514594125	0.34685036
6	mmu-miR-1298-3p	-0.7996	-0.8207	6.8865	5.03326286297947	0.56851062
7	mmu-miR-676-3p	-0.2493	0.7049	6.6387	4.78348080794851	0.69290686
8	mmu-miR-125a-5p	0.5267	0.1954	15.2271	4.6726950115645	0.70850929
9	mmu-miR-764-3p	-1.1463	-0.4890	4.6493	4.29117296787877	1.00000000
10	mmu-miR-187-3p	-0.2620	-1.1386	5.1092	4.10997964047295	1.00000000

Showing 1 to 10 of 1,966 entries Previous **1** 2 3 4 5 ... 197 Next

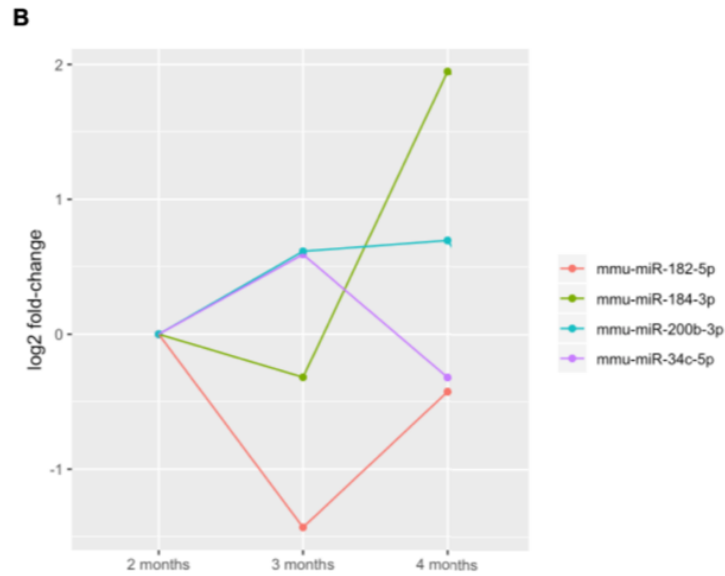


Fig. 11: Comparative analysis between PDGF mice (3- and 4-month-old) and all 2-month-old mice.

(A) 1966 miRNAs are identified in PDGF mice and the top 10 of miRNAs with small FDR value are shown. LogCPM, the log counts per million, is regarded as a parameter of assessing expression level for miRNAs. LogFC, the log fold change, represents difference between groups. Minus logFC means that miRNA is downregulated. FDR, the false discovery rate, is an adjust of p-value. miRNAs show significant difference when $FDR < 0.1$. (B) shows the fold changes of significantly altered miRNAs when compared 3- and 4-month-old PDGF to 2-month-old mice (PDGF and controls), $FDR < 0.1$.

Comparing 3- and 4-month-old PDGF to 2-month-old mice (PDGF and controls), the expression of mir-182-5p was reduced at 2 months of age compared to 3 months, followed by an increase from 3 to 4 months of age. The expression of mir-184-3p was reduced at 2 months compared to 3 months, followed by an increase from 3 to 4 months. The expression of mir-200-3p was ascending over time. The expression of mir-34c-5p was increased from 2 to 3-month, followed by a decrease from 3 to 4 months of age.

2.2.2.2 Differential expression of miRNAs in PDGF mice between each group (2, 3, 4 months)

For a more detailed analysis of miRNAs changes at different ages, a comparative analysis of miRNAs expression between PDGF mice at the age of 2, 3 and 4 months was performed.

2.2.2.2.1 Comparison between 3 and 2 months old PDGF mice

In order to identify miRNAs changes between 2 to 3 months old PDGF mice, a comparative analysis was performed between these two groups. It demonstrated that 7 miRNAs (mir-148a-3p, mir-34a-5p, mir-298-5p, mir-1298-5p, mir-676-3p, mir-132-5p and mir-1264-3p) showed significant difference in expression between 3- and 2-month-old PDGF mice (FDR < 0.1) (Figure 12).

	gene	logFC	logCPM	F	FDR
1	mmu-miR-148a-3p	-0.6423	12.4414	29.7935	0.00009493
2	mmu-miR-34a-5p	0.8896	6.9083	27.1023	0.00019042
3	mmu-miR-298-5p	-0.6748	8.7899	23.4818	0.00082881
4	mmu-miR-1298-5p	-0.7472	7.2470	20.6263	0.00274997
5	mmu-miR-676-3p	-0.7291	6.6387	16.7611	0.01669484
6	mmu-miR-132-5p	0.4971	9.9205	14.9974	0.03531976
7	mmu-miR-1264-3p	-1.2646	3.7360	13.3481	0.07272690
8	mmu-miR-133a-3p	0.5848	7.0147	12.1084	0.12345472
9	mmu-miR-193b-3p	0.9112	4.5168	11.1995	0.14774920
10	mmu-miR-674-5p	1.0385	3.9890	11.1731	0.14774920

Showing 1 to 10 of 1,966 entries Previous 1 2 3 4 5 ... 197 Next

Fig. 12: Differential expression of miRNAs between 3- and 2-month-old PDGF mice

The top 10 of 1966 identified miRNAs with the smallest FDR values are given. LogCPM, the log counts per million, is regarded as a parameter of assessing expression levels for miRNAs. LogFC, the log fold change, represents differences between groups. Minus logFC means that miRNA is downregulated. FDR, the false discovery rate, is an adjust of the p-value. miRNAs show significant difference when FDR < 0.1.

The results showed that mir-34a-5p and mir-132-5p were upregulated in 3-month-old PDGF mice, and mir-148a-3p, mir-298-5p, mir-1298-5p, mir-676-3p and mir-1264-3p were downregulated in 3-month-old PDGF mice compared to 3-month-old PDGF mice.

2.2.2.2.2 Comparison between 4 and 3 months old PDGF mice

In order to observe miRNAs changes in 4-month-old PDGF mice compared to 3-month-old ones, a miRNAs differential expression analysis was performed between these two groups. We observed that only mir-182-5p was upregulated in 4-month-old PDGF mice compared to 3-month-old PDGF mice (FDR < 0.1) (Figure 13).

	gene	logFC	logCPM	F	FDR
1	mmu-miR-182-5p	1.1312	9.2110	64.1522	0.00000000
2	mmu-miR-222-3p	0.4623	12.4469	14.4043	0.14512383
3	mmu-miR-34c-5p	-0.4844	9.4986	12.3919	0.24898146
4	mmu-miR-183-5p	0.7078	5.8900	11.8960	0.24898146
5	mmu-miR-138-5p	0.4053	13.4895	11.6303	0.24898146
6	mmu-miR-184-3p	0.7731	5.3925	11.3249	0.24898146
7	mmu-miR-598-3p	-0.5299	7.7442	11.0521	0.24898146
8	mmu-let-7e-5p	0.3850	12.7665	10.1943	0.34641345
9	mmu-miR-7013-5p	3.8272	1.3843	9.0655	0.56928563
10	mmu-miR-150-5p	0.3778	11.0684	8.7619	0.60500134

Showing 1 to 10 of 1,966 entries Previous 1 2 3 4 5 ... 197 Next

Fig. 13: Differential expression of miRNAs between 4- and 3-month-old PDGF mice

The top 10 of 1966 identified miRNAs with the smallest FDR values are given. LogCPM is the log counts per million, which is regarded as a parameter of assessing expression levels for miRNAs. LogFC, the log fold change, represents difference between groups. Minus logFC means that miRNA is downregulated. FDR, the false discovery rate, is an adjust of the p-value. miRNAs show significant difference when FDR < 0.1.

The results demonstrated that the miRNAs expression was barely different in 4-month-old compared to 3-month-old PDGF mice.

2.2.2.2.3 Comparison between 4 and 2 months old PDGF mice

Aim to double check the comparative results above, a comparative analysis was performed between 4- and 2-months-old PDGF mice. It was shown that 10 of miRNAs were significantly changed, namely mir-182-5p, mir-183-5p, mir-10b-5p, mir-132-3p, mir-1298-5p, mir-132-5p, mir-7a-5p, mir-298-5p, mir-770-5p and mir-34c-5p (FDR < 0.1) (Figure 14).

	gene	logFC	logCPM	F	FDR
1	mmu-miR-182-5p	1.1681	9.2110	75.8084	0.00000000
2	mmu-miR-183-5p	1.0129	5.8900	25.6585	0.00028095
3	mmu-miR-10b-5p	-0.7376	8.2591	25.5672	0.00028095
4	mmu-miR-132-3p	0.5493	11.7898	21.4654	0.00177508
5	mmu-miR-1298-5p	-0.7118	7.2470	18.8969	0.00543584
6	mmu-miR-132-5p	0.5515	9.9205	18.5060	0.00556013
7	mmu-miR-7a-5p	-1.2233	4.1745	16.8455	0.01140630
8	mmu-miR-298-5p	-0.5577	8.7899	16.2181	0.01389318
9	mmu-miR-770-5p	-0.8160	5.5699	14.7420	0.02695970
10	mmu-miR-34c-5p	-0.4645	9.4986	12.3039	0.08894136

Showing 1 to 10 of 1,966 entries Previous 1 2 3 4 5 ... 197 Next

Fig. 14: Differential expression of miRNAs between 4- and 2-month-old PDGF mice

The top 10 of 1966 identified miRNAs with the smallest FDR values are given. LogCPM is the log counts per million, which is regarded as a parameter of assessing expression level for miRNAs. LogFC, the log fold change, represents difference between groups. Minus logFC means that miRNA is downregulated. FDR, the false discovery rate, is an adjust of p-value. miRNAs show significant difference when FDR < 0.1.

Mir-182-5p, mir-183-5p, mir-132-3p and mir-132-5p were increased in 4-month-old compared to 2-month-old PDGF mice, and mir-10b-5p, mir-1298-5p, mir-7a-5p, mir-298-5p, mir-770-5p and mir-34c-5p were decreased in 4-onth-old compared to 2-months-old PDGF mice. The number of significantly changed miRNAs in the comparative analysis between 4 and 2 months old PDGF mice was more than in the comparative analysis between 3 and 2 (or 4 and 3) months old PDGF mice. Obviously

some slow but continuous miRNAs changes might occur that only become significant at 4 months of age.

DISCUSSION

PD is a common neurodegenerative disease which involves a damage of synapses throughout disease progression. The mechanism of altered synaptic function in PD is not yet understood but there is evidence that this relates to altered miRNA expression. Indeed, many miRNAs have been found to be associated with synaptic plasticity. However, they are not only involved in normal synapse formation and function but also in pathophysiology of PD (Ye et al., 2016) where altered synaptic plasticity has been proposed. As dendritic spine loss was observed in the neocortex of 3-month-old PDGF mice (Blumenstock et al., 2017), the hypothesis was put forward that the expression of some miRNAs may change between 2 and 3 months of age.

1. Differential expression of miRNAs between 2-month-old mice and the PDGF mice of 3 and 4 months of age

In order to validate this hypothesis, a comparative analysis was performed between 2 months PDGF plus control mice and 3- and 4-month-old PDGF mice. The results revealed that mir-184-3p, mir-182-5p, mir-34c-5p and mir-200b-3p were differentially expressed, which implied that these 4 miRNAs might mediate the dendritic loss in young PDGF mice.

The expression of mir-184-3p was reduced comparing 2 to 3 months old mice, followed by an increase comparing 3 to 4 months old mice. There is some evidence that mir-184 is involved in cognition and memory. Interestingly, changes in mir-184 expression have already been reported in neurodegenerative diseases that affect cognition. An *in vivo* study demonstrated mir-184 to be significantly downregulated in the hippocampus

of late-stage of AD, and it was verified that mir-184 was able to target NR4A2, which is found to be mediated cognition and long-term memory (Annese et al., 2018).

The expression of mir-182-5p was reduced comparing 2 to 3 months old mice, followed by an increase comparing 3 to 4 months old mice. Only a small number of studies on mir-182-5p associate this miRNA with memory. Actin (the major component of dendritic spines and is related to synaptic plasticity) and memory consolidation was regulated by mir-182-5p in male rat model (Fischer et al., 2004; Rex et al., 2010; Griggs et al., 2013). As synaptic plasticity is the cellular basis of memory, mir-182-5p was predicted to play a role in synaptic plasticity. The changes of mir-182-5p in PDGF mice was different from Griggs' findings, which might be due to the difference of the animal species and requires the furthermore studies.

The expression of mir-34c-5p was increased comparing 2 to 3-month-old mice, followed by a decrease comparing 3 to 4 months old mice. The mir-34 family miRNA is well studied in mammals. Mir-34b/c is mainly expressed in brain and lung tissue (Bommer et al., 2007). Mir-34 family members were considered to mediate tumor-suppressive effects (Li et al., 2009; Liu et al., 2011; Yamamura et al., 2012). Recently, there is some evidence that mir-34 may also be relevant for neurons. Downregulation of mir-34b/c has been found both at motor and pre-motor stages of PD patients' amygdala, frontal cortex, SN and cerebellum (Minones-Moyano et al., 2011). Mir-34 was found to be involved in neuronal differentiation in a drosophila model. In zebrafish, the silencing of mir-34 caused to the defect of neuronal development (Soni et al. 2013). Moreover, some *in vivo* evidence also confirmed that mir-34 mediate memory function.

A study demonstrated that the inhibition of mir-34 cause to an impaired reference memory in the Morris water maze (Malmevik et al., 2016).

The expression of mir-200b-3p was ascending over time in PDGF mice. Lately, the mir-200 family (including mir-200a, -200b, -200c, -141 and -429) has been found to be involved in neurodegenerative diseases. Increasing evidence has indicated that the miRNAs regulate proliferation, differentiation and apoptosis of neurons (Pandey et al., 2015; Trümbach et al., 2015). There are no reports of the role of mir-200 family in PD. But in Huntington's disease (HD), which is another neurodegenerative disease, an upregulation of mir-200a and mir-200c have been observed in the cortex and striatum of young HD mice. It was confirmed that the changes of mir-200a and mir-200c expression may affect neuronal plasticity and survival (Jin et al., 2012). Jin's finding implied that the mir-200 family might participate in neurodegenerative disease. The present study is the first one showing that this miRNA might also be relevant in PD.

2. Differential expression of miRNAs in PDGF mice between each group (2, 3, 4 months)

In order to get more insights on miRNAs' expression changes in PDGF mice at different ages, a comparative analysis between each PDGF group (2, 3 and 4 months of age) was performed. Besides mir-182-5p and mir-34c-5p changes similar to the results in the general assessment of miRNAs' differential expression, there were further 12 miRNAs that also showed significant changes, namely mir-148a-3p, mir-34a-5p, mir-298-5p, mir-1298-5p, mir-676-3p, mir-132-5p, mir-132-3p, mir-1264-3p, mir-183-5p, mir-10b-5p, mir-7a-5p and mir-770-5p. Among them, mir-148, mir-298, mir-1298, mir-

676, mir-1264, mir-183, mir-10 and mir-770 in neurodegenerative disorders are not known up to now. In contrast, the roles of mir-132 and mir-7 are well described.

The expression of mir-132 is known to be a critical factor in the development, maturation and function of neurons, and the dysregulation of this miRNA is associated with several neurodegenerative disorders (Wanet et al., 2012). The downregulation of mir-132 was found in AD patients. Mir-132 was reduced in the hippocampus, medial frontal gyrus, temporal and frontal cortex starting from the Braak stage III (Lau et al., 2010). This miRNA has also been identified to play an important role in the processing of synapse plasticity (Ye et al., 2016). However, the role of mir-132 in PD's pathogenesis is controversial: downregulation of mir-132 was observed in cortex and brainstem in 12-month-old (Thy1)-human α -syn (A30P)-transgenic mice (Gillardon et al., 2008). Whereas upregulation of mir-132 was identified in mesencephalon of a PD rat model (which is named Berlin-Druckrey IV (BD-IV) rats) at the age of 25 days (Lungu et al., 2013). Significant increase in the level of mir-132 was identified in PD patients (Alieva et al., 2015). The reasons for these conflicting results on mir-132 in PD are unknown and require further studies.

Mir-7 is regarded as a critical miRNA which participates in PD pathogenesis. An *in vitro* study reported that mir-7 reduces neurotoxicity and apoptotic nerve cell death caused by α -syn overexpression (Junn et al., 2009). Mir-7 was found to inhibit both α -syn aggregation and inflammasome activation. Moreover, it was found to restore impaired adult neurogenesis in the subventricular zone (Fan et al., 2016). The expression of mir-7 was shown to be decreased in young PDGF mice, which is consistent with Junn and Fan's findings. Interestingly, mir-7 was also found to prevent cell death (Kong et

al., 2009; Li et al., 2016). These results suggest that mir-7 might play an important role in PD.

In this study, more than 10 miRNAs in young PDGF mice were identified known to be involved in synaptic plasticity, however, the causal relationship between these miRNAs and synaptic dysfunction remain unclear. Here functional studies are needed analysis. Overexpressing, knockdown or knockout of these miRNAs in animal models of PD might help to understand if these miRNA's indeed affect synaptic plasticity. In 2011, Luikart downregulated mir-132 via stereotactic injections of a mir-132 sponge (bearing perfect binding sites for mir-132) in dentate gyrus to observe the expression of interleukin 6 (IL-6) in the granular neuronal layer of the adult mice hippocampus (Luikart et al., 2011). A mir-182 knockout mouse has been recently generated for studying the role of this miRNA in the retina (Jin et al., 2009), which might be useful in further studies in a PD related context.

In conclusion, we identified that more than 10 miRNAs that were significantly changed in young PDGF mice at an age when dendritic spine loss occurs, especially mir-184-3p, mir-182-5p, mir-34c-5p, mir-200b-3p, mir-132-5p and mir-7a-5p. This observation implies that these miRNAs might play an important role in cognitive changes that can be observed in about 80% of PD patients throughout the progression of the disease. Nevertheless, there were controversy in the expression and role of mir-132-5p, which have to be studied furthermore. In addition, the verification of miRNAs expression level by qPCR, the analysis of miRNAs potential downstream target genes and the miRNA's function analysis will need to be done in future studies. However, the present study establishes for the first time a list of miRNAs alterations in a mouse model of PD that

coincides with the loss of dendritic spines. It provides important insights how miRNA might affect synaptic function in the cerebral cortex in the context of α -synuclein aggregation and suggests for further investigations aimed at better understanding the molecular mechanisms in PD.

REFERENCE

- Alieva AKh, Filatova EV, Karabanov AV, Illarioshkin SN, Limborska SA, Shadrina MI, Slominsky PA. (2015). miRNA expression is highly sensitive to a drug therapy in Parkinson's disease. *Parkinsonism Relat Disord.* 21(1):72-4.
- Amschl D, Neddens J, Havas D, Flunkert S, Rabl R, Römer H, Rockenstein E, Masliah E, Windisch M, Hutter-Paier B. (2013). Time course and progression of wild type α -synuclein accumulation in a transgenic mouse model. *BMC Neurosci.* 14:6.
- Annese A, Manzari C, Lionetti C, Picardi E, Horner DS, Chiara M, Caratozzolo MF, Tullo A, Fosso B, Pesole G, D'Erchia AM. (2018). Whole transcriptome profiling of Late-Onset Alzheimer's Disease patients provides insights into the molecular changes involved in the disease. *Sci Rep.* 8(1):4282.
- Aron L, Klein R. (2010). Repairing the parkinsonian brain with neurotrophic factors. *Trends Neurosci.* 34(2):88-100.
- Blumenstock S, Rodrigues EF, Peters F, Blazquez-Llorca L, Schmidt F, Giese A, Herms J. (2017). Seeding and transgenic overexpression of alpha-synuclein triggers dendritic spine pathology in the neocortex. *EMBO Mol Med.* 2017 May;9(5):716-731.
- Boese AS, Saba R, Campbell K, Majer A, Medina S, Burton L, Booth TF, Chong P, Westmacott G, Dutta SM, Saba JA, Booth SA. (2016). MicroRNA abundance is altered in synaptoneuroosomes during prion disease. *Mol Cell Neurosci.* 71:13-24.
- Bommer GT, Gerin I, Feng Y, Kaczorowski AJ, Kuick R, Love RE, Zhai Y, Giordano TJ, Qin ZS, Moore BB, MacDougald OA, Cho KR, Fearon ER. (2007). p53-mediated activation of miRNA34 candidate tumor-suppressor genes. *Curr Biol.* 17(15):1298-307.
- Burré J, Sharma M, Tsetsenis T, Buchman V, Etherton MR, Südhof TC. (2010). Alpha-synuclein promotes SNARE-complex assembly in vivo and in vitro. *Science.* 329(5999):1663-7.
- Calo L, Wegrzynowicz M, Santivañez-Perez J, Grazia Spillantini M. (2016). Synaptic failure and α -synuclein. *Mov Disord.* 31(2):169-77.

- Cattell RB. (1966). The Scree Test for The Number of Factors. *Multivariate Behav Res.* 1(2):245-76.
- Chédotal A. (2011). Further tales of the midline. *Curr. Opin. Neurobiol.* 21(1):68-75.
- Chen Y, Lun AT, Smyth GK. (2016). From reads to genes to pathways: differential expression analysis of RNA-Seq experiments using Rsubread and the edgeR quasi-likelihood pipeline. Version 2. *F1000Res.* 5:1438.
- Chesselet MF, Fleming S, Mortazavi F, Meurers B. (2008). Strengths and limitations of genetic mouse models of Parkinson's disease. *Parkinsonism Relat Disord.* 14 (Suppl 2): S84-7.
- Choi DC, Yoo M, Kabaria S, Junn E. (2018). MicroRNA-7 facilitates the degradation of alpha-synuclein and its aggregates by promoting autophagy. *Neurosci Lett.* 678:118-123.
- Cilia R, Tunesi S, Marotta G, Cereda E, Siri C, Tesei S, Zecchinelli AL, Canesi M, Mariani CB, Meucci N, Sacilotto G, Zini M, Barichella M, Magnani C, Duga S, Asselta R, Soldà G, Seresini A, Seia M, Pezzoli G, Goldwurm S. (2016). Survival and dementia in GBA-associated Parkinson's disease: The mutation matters. *Ann Neurol.* 80(5):662-673.
- DeKosky ST1, Scheff SW, Styren SD. (1996). Structural correlates of cognition in dementia: quantification and assessment of synapse change. *Neurodegeneration.* 5(4):417-21.
- Doepfner TR, Doehring M, Bretschneider E, Zechariah A, Kaltwasser B, Müller B, Koch JC, Bähr M, Hermann DM, Michel U. (2013). MicroRNA-124 protects against focal cerebral ischemia via mechanisms involving Usp14-dependent REST degradation. *Acta Neuropathol.* 126(2):251-65.
- Doty RL. (2012). Olfactory dysfunction in Parkinson disease. *Nat Rev Neurol.* 8(6):329-39.
- Emre M1, Aarsland D, Brown R, Burn DJ, Duyckaerts C, Mizuno Y, Broe GA, Cummings J, Dickson DW, Gauthier S, Goldman J, Goetz C, Korczyn A, Lees A, Levy R, Litvan I, McKeith I, Olanow W, Poewe W, Quinn N, Sampaio C, Tolosa E, Dubois

- B. (2007). Clinical diagnostic criteria for dementia associated with Parkinson's disease. *Mov Disord.* 22(12):1689-707.
- Fan Z, Lu M, Qiao C, Zhou Y, Ding JH, Hu G. (2016). MicroRNA-7 Enhances Subventricular Zone Neurogenesis by Inhibiting NLRP3/Caspase-1 Axis in Adult Neural Stem Cells. *Mol Neurobiol.* 53(10):7057-7069.
- Fernagut PO, Chesselet MF. (2004). Alpha-synuclein and transgenic mouse models. *Neurobiol Dis.* 17(2):123-30.
- Fischer A, Sananbenesi F, Schrick C, Spiess J, Radulovic J. (2004). Distinct roles of hippocampal de novo protein synthesis and actin rearrangement in extinction of contextual fear. *J Neurosci.* 24(8):1962-6.
- Fleming SM, Salcedo J, Fernagut PO, Rockenstein E, Masliah E, Levine MS, Chesselet MF. (2004). Early and progressive sensorimotor anomalies in mice overexpressing wild-type human alpha-synuclein. *J Neurosci.* 24(42):9434-40.
- Fleming SM, Tetreault NA, Mulligan CK, Hutson CB, Masliah E, Chesselet MF. (2008). Olfactory deficits in mice overexpressing human wildtype alpha-synuclein. *Eur J Neurosci.* 28(2):247-56.
- Gehrke S, Imai Y, Sokol N, Lu B. (2010). Pathogenic LRRK2 negatively regulates microRNA-mediated translational repression. *Nature.* 466(7306):637-41.
- Gillardon F, Mack M, Rist W, Schnack C, Lenter M, Hildebrandt T, Hengerer B. (2008). MicroRNA and proteome expression profiling in early-symptomatic α -synuclein(A30P)-transgenic mice. *Proteomics Clin Appl.* 2(5):697-705.
- Griggs EM, Young EJ, Rumbaugh G, Miller CA. (2013). MicroRNA-182 regulates amygdala-dependent memory formation. *J Neurosci.* 33(4):1734-40.
- Hoss AG, Labadorf A, Beach TG, Latourelle JC, Myers RH. (2016). microRNA Profiles in Parkinson's Disease Prefrontal Cortex. *Front Aging Neurosci.* 8:36.
- Jan Christoph Koch, Mathias Bähr, Paul Lingor. (2012). Targeting neurological disease with siRNA. *Controlled Genetic Manipulations.* Springer. pp. 97–111.
- Jin J, Cheng Y, Zhang Y, Wood W, Peng Q, Hutchison E, Mattson MP, Becker KG, Duan W. (2012). Interrogation of brain miRNA and mRNA expression profiles reveals

a molecular regulatory network that is perturbed by mutant huntingtin. *J Neurochem.* 123(4):477-90.

Jin ZB, Hirokawa G, Gui L, Takahashi R, Osakada F, Hiura Y, Takahashi M, Yasuhara O, Iwai N. (2009). Targeted deletion of miR-182, an abundant retinal microRNA. *Mol Vis.* 15:523–533.

Junn E, Lee KW, Jeong BS, Chan TW, Im JY, Mouradian MM. (2009). Repression of alpha-synuclein expression and toxicity by microRNA-7. *Proc Natl Acad Sci U S A.* 106(31):13052-7.

Kabiri Rad H, Mazaheri M, Dehghani Firozabadi A. (2018). Relative Expression of PBMC MicroRNA-133a Analysis in Patients Receiving Warfarin After Mechanical Heart Valve Replacement. *Avicenna J Med Biotechnol.* 10(1):29-33.

Khodadadian A, Hemmati-Dinarvand M, Kalantary-Charvadeh A, Ghobadi A, Mazaheri M. (2018). Candidate biomarkers for Parkinson's disease. *Biomed Pharmacother.* 104:699-704.

Kim J, Inoue K, Ishii J, Vanti WB, Voronov SV, Murchison E, Hannon G, Abeliovich A. (2007). A MicroRNA feedback circuit in midbrain dopamine neurons. *Science.* 317(5842):1220-4.

Kingwell K. (2017). Zeroing in on neurodegenerative α -synuclein. *Nat Rev Drug Discov.* 16(6):371-373.

Kong W, Zhao JJ, He L, Cheng JQ. (2009). Strategies for profiling microRNA expression. *J Cell Physiol.* 18(1):22-5.

Lau P, de Strooper B. (2010). Dysregulated microRNAs in neurodegenerative disorders. *Semin Cell Dev Biol.* 21(7):768-73.

Lee RC, Feinbaum RL, Ambros V. (1993) The *C. elegans* heterochronic gene *lin-4* encodes small RNAs with antisense complementarity to *lin-14*. *Cell.* 75(5):843-54.

Leggio L, Vivarelli S, L'Episcopo F, Tirolo C, Caniglia S, Testa N, Marchetti B, Iraci N. (2017). microRNAs in Parkinson's Disease: From Pathogenesis to Novel Diagnostic and Therapeutic Approaches. *Int J Mol Sci.* 18(12). pii: E2698.

- Lewis S. (2014). Neurological disorders: microRNA gets motoring. *Nat Rev Neurosci.* 15(2):67.
- Li S, Lv X, Zhai K, Xu R, Zhang Y, Zhao S, Qin X, Yin L, Lou J. (2016). MicroRNA-7 inhibits neuronal apoptosis in a cellular Parkinson's disease model by targeting Bax and Sirt2. *Am J Transl Res.* 8(2):993-1004.
- Li Y, Guessous F, Zhang Y, Dipierro C, Kefas B, Johnson E, Marcinkiewicz L, Jiang J, Yang Y, Schmittgen TD, Lopes B, Schiff D, Purow B, Abounader R. (2009). MicroRNA-34a inhibits glioblastoma growth by targeting multiple oncogenes. *Cancer Res* 69:7569–7576.
- Liu C, Kelnar K, Liu B, Chen X, Calhoun-Davis T, Li H, Patrawala L, Yan H, Jeter C, Honorio S, Wiggins JF, Bader AG, Fagin R, Brown D, Tang DG. (2011). The microRNA miR-34a inhibits prostate cancer stem cells and metastasis by directly repressing CD44. *Nat Med* 17:211–215.
- Liu J, Zhou Y, Wang C, Wang T, Zheng Z, Chan P. (2012). Brain-derived neurotrophic factor (BDNF) genetic polymorphism greatly increases risk of leucine-rich repeat kinase 2 (LRRK2) for Parkinson's disease. *Parkinsonism Relat Disord.* 18(2):140-3.
- Luikart BW, Bensen AL, Washburn EK, Perederiy JV, Su KG, Li Y, Kernie SG, Parada LF, Westbrook GL. (2011) miR-132 mediates the integration of newborn neurons into the adult dentate gyrus. *PLoS One.* 6(5): e19077.
- Lungu G, Stoica G, Ambrus A. (2013). MicroRNA profiling and the role of microRNA-132 in neurodegeneration using a rat model. *Neurosci Lett.* 553:153-8.
- Malmevik J, Petri R, Knauff P, Brattås PL, Åkerblom M, Jakobsson J. (2016). Distinct cognitive effects and underlying transcriptome changes upon inhibition of individual miRNAs in hippocampal neurons. *Sci Rep.* 6:19879.
- Maries E, Dass B, Collier TJ, Kordower JH, Steece-Collier K. (2003). The role of alpha-synuclein in Parkinson's disease: insights from animal models. *Nat Rev Neurosci.* 4(9):727-38.
- Maroteaux L, Campanelli JT, Scheller RH. (1988). Synuclein: a neuron-specific protein localized to the nucleus and presynaptic nerve terminal. *J Neurosci.* 8(8):2804-15.

Masliah E, Rockenstein E, Veinbergs I, Mallory M, Hashimoto M, Takeda A, Sagara Y, Sisk A, Mucke L. (2000). Dopaminergic loss and inclusion body formation in alpha-synuclein mice: implications for neurodegenerative disorders. *Science*. 287(5456):1265-9.

Mellios N, Sugihara H, Castro J, Banerjee A, Le C, Kumar A, Crawford B, Strathmann J, Tropea D, Levine SS, Edbauer D, Sur M. (2011). miR-132, an experience-dependent microRNA, is essential for visual cortex plasticity. *Nat. Neurosci*. 14(10), 1240-1242.

Meza-Sosa KF, Pedraza-Alva G, Pérez-Martínez L. (2014). microRNAs: key triggers of neuronal cell fate. *Front Cell Neurosci*. 8:175.

Miñones-Moyano E, Porta S, Escaramís G, Rabionet R, Iraola S, Kagerbauer B, Espinosa-Parrilla Y, Ferrer I, Estivill X, Martí E. (2011). MicroRNA profiling of Parkinson's disease brains identifies early downregulation of miR-34b/c which modulate mitochondrial function. *Hum Mol Genet*. 20(15):3067-78.

Nadim WD, Simion V, Benedetti H, Pichon C, Baril P, Morisset-Lopez S. (2017). MicroRNAs in Neurocognitive Dysfunctions: New Molecular Targets for Pharmacological Treatments? *Curr Neuropharmacol*. 15(2):260-275.

Pandey A, Singh P, Jauhari A, Singh T, Khan F, Pant AB, Parmar D, Yadav S. (2015). Critical role of the miR-200 family in regulating differentiation and proliferation of neurons. *J Neurochem*. 133(5):640-52.

Rex CS, Gavin CF, Rubio MD, Kramar EA, Chen LY, Jia Y, Haganir RL, Muzyczka N, Gall CM, Miller CA, Lynch G, Rumbaugh G. (2010). Myosin IIb regulates actin dynamics during synaptic plasticity and memory formation. *Neuron*. 67(4):603-17.

Robinson MD, McCarthy DJ, Smyth GK. (2010). edgeR: a Bioconductor package for differential expression analysis of digital gene expression data. *Bioinformatics*. 26(1):139-40.

Rockenstein E, Mallory M, Hashimoto M, Song D, Shults CW, Lang I, Masliah E. (2002). Differential neuropathological alterations in transgenic mice expressing alpha-synuclein from the platelet-derived growth factor and Thy-1 promoters. *J Neurosci Res*. 68(5):568-78.

- Sayed D, Abdellatif M. (2011). MicroRNAs in development and disease. *Physiol Rev.* 91(3):827-87.
- Sherer TB. (2011). Biomarkers for Parkinson's disease. *Sci Transl Med.* 3(79):79ps14.
- Smith PK, Krohn RI, Hermanson GT, Mallia AK, Gartner FH, Provenzano MD, Fujimoto EK, Goeke NM, Olson BJ, Klenk DC. (1985). Measurement of protein using bicinchoninic acid. *Anal Biochem.* 150(1): 76-85.
- Snead D, Eliezer D. (2014). Alpha-synuclein function and dysfunction on cellular membranes. *Exp Neurobiol.* 23(4):292-313.
- Soni K, Choudhary A, Patowary A, Singh AR, Bhatia S, Sivasubbu S, Chandrasekaran S, Pillai B. (2013). miR-34 is maternally inherited in *Drosophila melanogaster* and *Danio rerio*. *Nucleic Acids Res* 41: 4470–4480.
- Trümbach D, Prakash N. (2015). The conserved miR-8/miR-200 microRNA family and their role in invertebrate and vertebrate neurogenesis. *Cell Tissue Res.* 359(1):161-77.
- Wanet A, Tacheny A, Arnould T, Renard P. (2012). miR-212/132 expression and functions: within and beyond the neuronal compartment. *Nucleic Acids Res.* 40(11):4742-53.
- Yamamura S, Saini S, Majid S, Hirata H, Ueno K, Chang I, Tanaka Y, Gupta A, Dahiya R. (2012). MicroRNA-34a suppresses malignant transformation by targeting c-Myc transcriptional complexes in human renal cell carcinoma. *Carcinogenesis* 33:294–300.
- Ye Y, Xu H, Su X, He X. (2016). Role of MicroRNA in Governing Synaptic Plasticity. *Neural Plast.* 2016:4959523.
- Zimprich A, Benet-Pagès A, Struhal W, Graf E, Eck SH, Offman MN, Haubenberger D, Spielberger S, Schulte EC, Lichtner P, Rossle SC, Klopp N, Wolf E, Seppi K, Pirker W, Presslauer S, Mollenhauer B, Katzenschlager R, Foki T, Hotzy C, Reinthaler E, Harutyunyan A, Kralovics R, Peters A, Zimprich F, Brücke T, Poewe W, Auff E, Trenkwalder C, Rost B, Ransmayr G, Winkelmann J, Meitinger T, Strom TM. (2011). A mutation in VPS35, encoding a subunit of the retromer complex, causes late-onset Parkinson disease. *Am J Hum Genet.* 89(1):168-75.

ABBREVIATION

°C	degree celcius
µg	microgram
APS	Ammonium persulphate solution
BCA	Bicinchoninic Acid
bp	base pair
cDNA	complementary DNA
CPM	counts per million
CREB	cAMP Response Element-binding Protein
DA	Dopaminergic
dNTP	Deoxynucleoside triphosphate
dsDNA	double strand DNA
DTT	Dithiothreitol
e.g.	for example
EAAT2	Excitatory Amino Acid Transporter 2
ECL	Enhanced chemiluminescence
EDTA	Ethylenediaminetetraacetic acid
F	female
FC	Fold Change
FDR	False discovery rate
Fig.	Figure
g	gram
Gbp	Giga base pairs
h	hour
HCl	hydrochloride
HD	Huntington's disease
IL-6	Interleukin 6
kDa	kilodalton
LRRK2	Leucine Rich Repeat Kinase 2
M	male
mg	milligram

MgCl ₂	Magnesium chloride
min	minute
miRNA	microRNA
ml	milliliter
mM	millimolar
N	mol
NaCl	Sodium chloride
NaOH	Sodium hydroxide
NEM	N-Ethylmaleimide
ng	nanogram
nM	nanomolar
No.	number
NP	Nonidet P-40
nt	nucleotide
PAGE	Polyacrylamide Gel Electrophoresis
PCA	Principal Component Analysis
PCR	Polymerase Chain Reaction
PD	Parkinson's disease
PDD	Parkinson's disease Dementia
PFA	Paraformaldehyde
pM	picomolar
PMSF	Phenylmethylsulfonyl Fluorid
pre-miRNA	precursor miRNA
pri-miRNA	primary microRNA
PVDF	Polyvinylidene Difluoride
RISC	RNA-induced silencing complex
RNase	Ribonuclease
rpm	revolutions per minute
RSB	Resuspension Buffer
RT	Room Temperature
SDS	Sodium Dodecyl Sulfate
Sec	second
SNpc	substantia nigra pars compacta

TAE	Tris-acetate-EDTA
TBS	Tris-Buffered Saline
TBST	Tris Buffered Saline with Tween 20
Temed	Tetramethylethylenediamine
Tris	THAM, Tris (hydroxymethyl) aminomethane
UPS	Ubiquitin Proteasome System
UV	Ultraviolet
V	volt
WB	western blot
μl	microliter
α-syn	alpha-synuclein

ACKNOWLEDGEMENT

First of all, I would like to express my gratitude to my supervisor Prof. Dr. Jochen Herms, for giving me the chance to work in his lab and providing me with the interesting and challenging project of my thesis. Thank you very much for your great supervision, for always taking time to discuss and for all the things I could learn from you during the last years.

I furthermore want to cordially thank Dr. Otto Windl, who provides useful advices about my research project and assistance in writing reports. Thank you so much for your patience all the time. I am benefited a lot from your scientific thinking and wealthy knowledge.

I would like to thank Dr. Felix Strübing for great help. I appreciate your vast knowledge and skills in many areas. I must also acknowledge Dr. Carmelo Sgobio, Dr. Gerda Mitteregger, Dr. Daniel Weckbecker, Jose Medina Luque, Dr. med. Meike Miller, Virginie Guibourt, Andrea Greiner, Martin Bartels, Jeannine Widmann, Viktoria Ruf, Dr. Felix Schmidt, Yuan Shi, Fanfan Sun and for their valuable suggestions and useful discussion. Furthermore, acknowledge must give to the excellent technical support provided by Fang Zhang, Nadine Lachner, Janina Mielke and Michael Rüter.

Several collaborators have provided me with material or the possibility to share thoughts and learn. I furthermore want to acknowledge all second readers of this thesis for your time and interest in this work.

Last but not least, thanks to my family: my husband, my parents and my son. Thanks for all the love and support coming from them.